Vol. 15, No. 1 (2026): 153 - 163 http://dx.doi.org/10.23960/jtepl.v15i1.153-163

JURNAL TEKNIK PERTANIAN LAMPUNG

ISSN 2302-559X (print) / 2549-0818 (online)
Journal homepage : https://jurnal.fp.unila.ac.id/index.php/JTP

Design and Performance Evaluation of an IoT-Based Automatic Airflow Control System for a PV/T Solar Dryer with Silica Gel Adsorption Heat Storage

Putri Arsyafdini Oktavionry[1,✉], Leopold Oscar Nelwan[1], I Dewa Made Subrata[1]

[1] Department of Mechanical and Biosystems Engineering, Faculty of Agricultural Technology, IPB University, Bogor, INDONESIA.

Article History:

Received : 27 October 2025
Revised : 21 January 2026
Accepted : 22 January 2026

Keywords:

Adsorption,
Drying,
Energy,
Photovoltaic-collector.

Corresponding Author:
✉ putri20arsyafdini@apps.ipb.ac.id
(Putri Arsyafdini Oktavionry)

ABSTRACT

Solar energy is one of the most promising renewable energy sources, yet solar drying operating costs often remain prohibitive for small-scale farming. This research aims to design and evaluate the performance of an automated air flow control system for a PV/T collector integrated with an adsorption channel. The methodology focuses on developing a real-time monitoring and control logic based on environmental parameters. The system utilizes a microcontroller-based unit for data acquisition of temperature and humidity, coupled with a high-torque motor actuation system to regulate valve positioning between the collector and the desiccant unit. Results indicate that the control system manages air distribution effectively across a temperature control range of 40 °C to 4 3°C. The system demonstrated high responsiveness with a mechanical actuation speed of 3 seconds for a full 90-degree valve rotation. During the adsorption phase, the silica gel's moisture content rose from 23.57% to 27.38%. Furthermore, the silica gel adsorption unit contributed to thermal stability by maintaining a temperature gradient of 3-7 °C between the plenum and the environment, effectively recycling adsorption heat to enhance the drying air temperature even during low solar radiation.

1. INTRODUCTION

Solar energy is considered one of the most promising renewable energy sources. The conversion through Photovoltaic Thermal (PV/T) technology has been proven to significantly increase energy efficiency (Kong *et al*., 2020; Ludin *et al*., 2018; Santika *et al*., 2019). Solar PV/T collectors are capable of collecting solar radiation energy and converting it into thermal energy to provide sufficient heat for drying and electrical energy (Putra *et al*., 2019; Samykano, 2023). In this study, a PV-T system and solar collector for drying agricultural products are proposed (Kazem *et al*., 2023; Tonadi *et al*., 2024). The main challenges of solar-powered drying systems lie in the instability of energy supply and the risk of humid air wetting the products. One solution to overcome this problem is to use silica gel as an adsorbent (Rambhad *et al*., 2023). Silica gel not only aids in mass and heat transfer (Jimoh *et al*., 2023), but also functions as a heat storage medium (Ayisi & Fraňa, 2020; Mitran *et al*., 2021). Unlike sensible media such as water, which is prone to heat loss, silica gel stores energy through adsorption, resulting in very little static heat loss and enabling long-term energy storage (Ayaz *et al*., 2021).

The research gap addressed in this study lies in the integration of real-time environmental monitoring with an automated decision-making system for PV/T-adsorption drying. While previous studies, such as Nelwan *et al*. (2024), successfully utilized adsorption storage but relied on manual operation, and Khalil *et al*. (2016) used basic thermal triggers for water-based storage, but there has been no research on IoT-integrated systems that can dynamically switch

between solar-thermal and adsorption-heat modes based on instantaneous RH and temperature changes. In contrast to these existing studies, this research introduces an automated airflow control system that eliminates manual intervention and optimizes heat recovery from the adsorption process. This provides a more robust solution to the instability of solar energy, ensuring a stable drying temperature even during low-radiation periods.

This research aims to design and evaluate an automated, decision-logic-based control system for a PV/T solar dryer integrated with a silica gel adsorption channel. By processing real-time multi-sensor data, the system optimizes airflow management to maximize heat storage and silica gel regeneration. This approach ensures consistent drying efficiency and effectively mitigating energy supply instabilities during periods of low-to-moderate solar radiation.

2. MATERIALS AND METHODS

This research was conducted at the Instrumentation and Control Laboratory and the Renewable Energy Laboratory, Department of Mechanical and Biosystems Engineering, Faculty of Agricultural Technology, IPB University.

2.1. Tools and Materials

The main material used in this study was 24 kg of silica gel. The tools used in this study consisted of equipment for testing the control system included a dryer and a pyranometer. In addition, equipment for creating a control system circuit included jumper cables, AWG cables, blowers, DHT22 sensors, ESP32 Wroom, expansion board shields, DC worm gear boxes with high torque, BTS7960-43A high power motor driver modules, Dservo DS3225 metal gear high torque, duct volume dampers, 12V power supplies, 2-channel relays, and computer software.

2.2. Research Procedures

This research consisted of three stages, namely: (1) Creating a control system circuit, which includes compiling a system flow chart, creating modules, and calibrating sensors; (2) Testing the control system on the solar collector and adsorption dryer; and (3) Analyzing and processing data to determine the performance of the control system in the drying process.

2.3. Solar Drying System

This drying machine uses a tray-type dryer with a solar collector and adsorption. The parts of the drying machine are a photovoltaic collector, a drying tub, and a silica gel tank for heat storage. The overall system and the drying machine with a solar collector and heat storage can be seen in Figure 1. In this study, the control system is the main component for controlling the drying and heat storage processes. The role of the control system is to control the actuators, which consist of seven valves and two blowers. The control process is carried out based on the readings from the temperature and humidity sensors, which are detected and then processed by a microcontroller, and the readings result are sent to a Google spreadsheet. Figure 2 illustrates the air flow in the drying system.

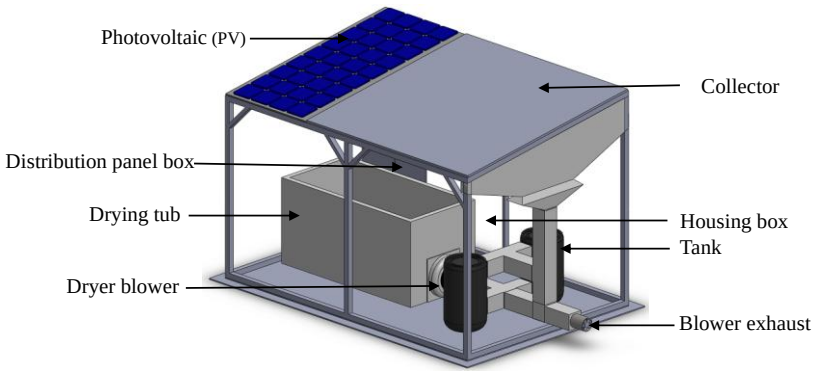

Figure 1. Drying machine with solar collector and heat storage

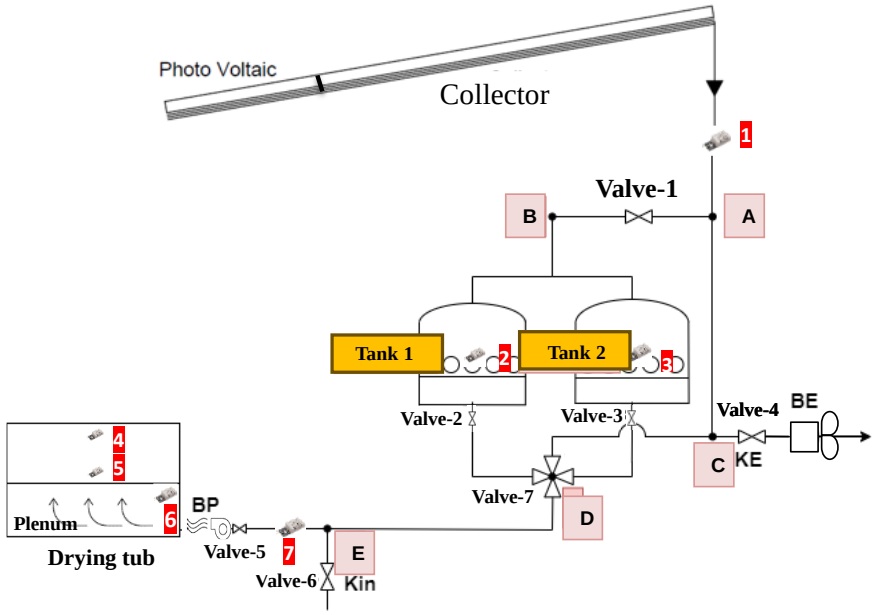

Figure 2. Schematic diagram of a dryer with a solar collector and heat storage unit

Table 1. Air flow diagram of the drying system

Air flow	Scheme	Opened Valve
1	PV/T-Collector-A-C-D-E-Drying Tub	7 and 5
2	PV/T-Collector-A-B-Tank 1 and 2	1,7, and 5
3	Tank 1 or 2-D-E-Drying Tub	2 or 3, and 5
4	Tank 1 or 2-D-C-Blower Exhaust	2 or 3, 7, 4, and 5
5	E-Drying Tub	6 and 5

The air flow diagram for this system can be seen in Table 1 showing the first air flow, which transfers heat directly from the photovoltaic collector to the drying chamber. The second air flow transfers heat from the collector to the drying chamber and to the silica gel tanks (1 and 2) through valve 1. In the third air flow, if the heat from the collector decreases, valve-1 will close, then the stored heat is released sequentially: valve-2 opens to use tank 1, and after it is empty, valve-3 opens to transfer heat from tank 2. The fourth air flow is used for silica gel regeneration using a blower; in this process, valve 4 opens and the blower turns on until the silica moisture content returns to normal. The fifth air flow involves valve 6, which opens when sensor 7 reads a temperature below 43 °C, while valve 5 remains open during the drying process. Valve 7 functions to regulate air flow at position K.7.1 with a rotation angle of 45°, K.7.2 with a rotation angle of 135°, and K.7.3 with a rotation angle of 90° in the control system schematic diagram of the dryer with a solar collector and adsorption, as shown in Figure 3 and Valve position at point 7 can be seen in Figure 1. Therefore, Table 1 shows that air flows 1, 3, and 5, 1 and 2, and 3 and 4 can occur simultaneously.

Figure 3 clearly shows that the air flow in this drying system is dynamic and determined by an automatic control system based on operational requirements. The air flow is not static but can occur under several conditions because the control system intelligently activates the actuator according to the detected parameters. For example, when the equilibrium water content (M_e) T1 (tank 1) is lower than M_e plenum, the system will open valve 2 to flow dry air into the drying chamber. This proves that the air flow is managed precisely based on programmed control logic.

The temperature and humidity data read by the sensor is converted into equilibrium water content (M_e) for control purposes using Equation 1. Equation 1 is used to measure air conditions at all points in order to simplify and focus the control logic on product quality. When comparing different units, the system converts air temperature and humidity into M_e, allowing the system to directly compare the potential water absorption capacity of the air at one location to another.

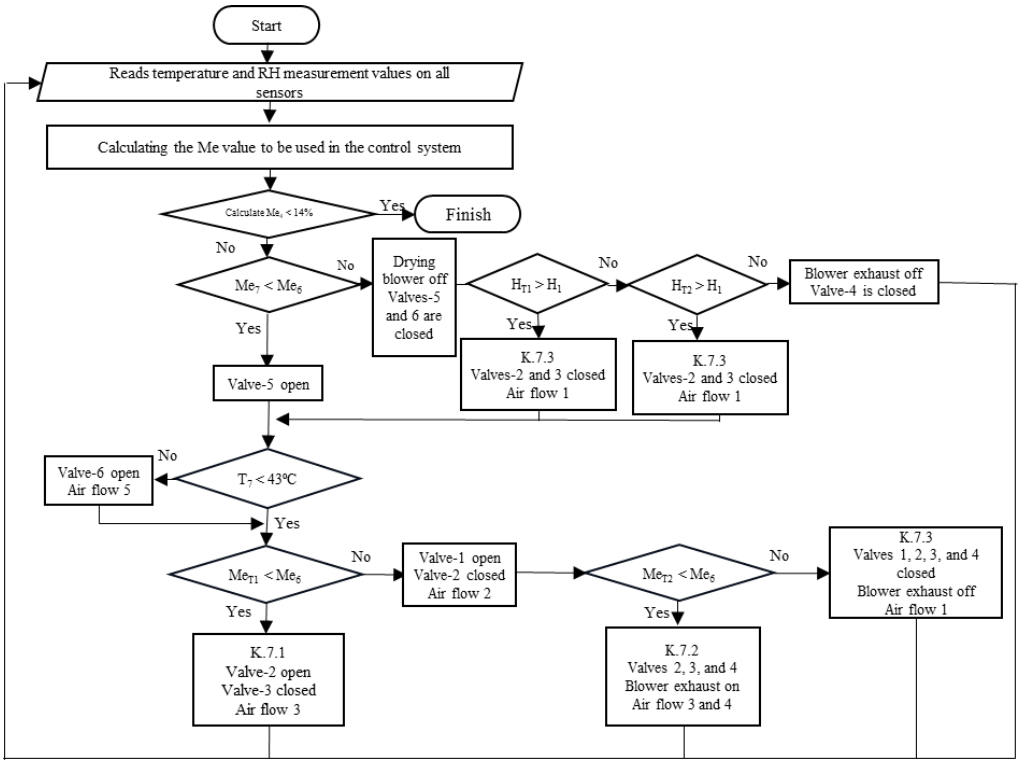

Figure 3. Control system diagram for a dryer with solar collector and adsorption

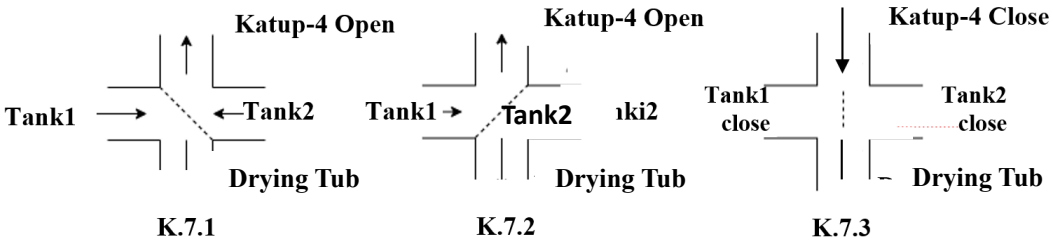

Figure 4. Valve position at point 7

The equilibrium water content equation is based on Henderson (Thomson, 1967) in (Sadaka, 2022). The constants K, C, and N in the Henderson equation are empirical product constants specific to the material being dried (grain).

$$M_e = \left[\frac{\ln(1 - RH)}{-K(1.8 \times T + C)}\right]^{1/N} \quad (1)$$

where M_e is dry basis equilibrium moisture content (% d.b), RH is relative humidity (%), T is absolute air temperature expressed in (C), K (grain) is 4.726×10^{-6}, C (grain) is 491.7, and N (grain) = 2.386.

The automated control and data acquisition system operates through an ESP32 microcontroller-based software designed for real-time monitoring and operational regulation. As illustrated in Figure 5, the control mechanism detects critical parameters, including temperature, relative humidity, and equilibrium moisture content (M_e) calculated via the Henderson equation. These sensor inputs are processed to execute precise commands for actuators specifically servo motors, DC motors, and blowers to optimize airflow distribution. Beyond simple connectivity, the ESP32 serves as a critical gateway for real-time data synchronization with a Google Spreadsheet, ensuring high data integrity by eliminating manual logging errors and enabling continuous remote oversight via smartphones or laptops. The overall system of the dryer with a solar collector and heat storage can be seen in Figure 6.

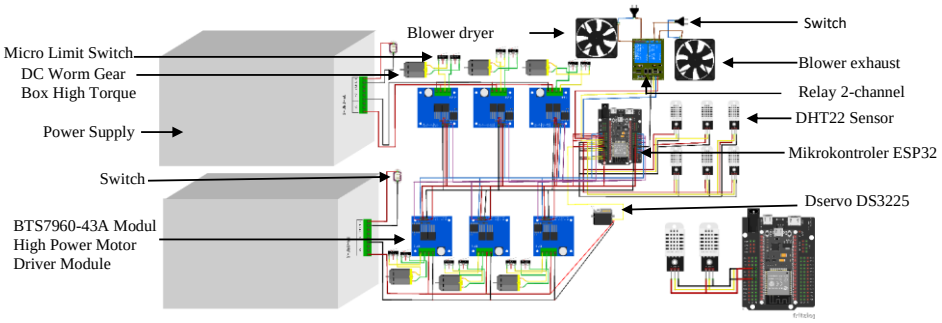

Figure 5. Control system diagram

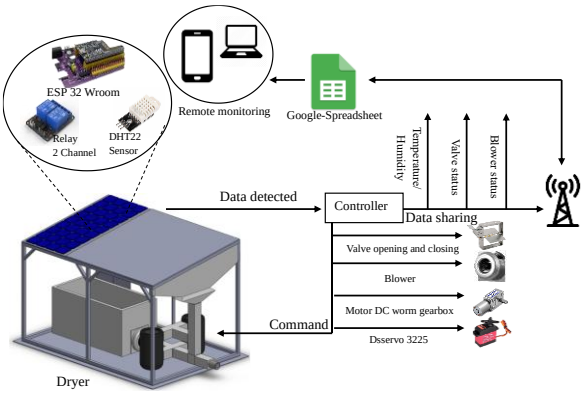

Figure 6. Overall system of the dryer with solar collector and heat storage

2.4. Data Collection

Data collection was conducted from 8:00 a.m. to 5:00 p.m. for three days. The data collected in this observation included temperature, humidity, and equilibrium moisture content in the dryer using a control system with data transmission every 10 seconds. The data was then processed further every 5 min. Solar radiation data was collected using a pyranometer.

2.5. Data Analysis

2.5.1. Control System Performance Test

Testing for system performance was conducted to evaluate the performance of integrated control and mechanical components in achieving efficient drying objectives. This step included monitoring and controlling air temperature and humidity of the dryer, and observation water content changes in the silica gel. The first was conducted to monitor the distribution of dryer air temperature and humidity occurring in the drying machine. The purpose is to observe temperature fluctuations that occur from the start of the system operation until the end. The changes in silica gel water content was performed to determine the time required to detect changes in silica gel water content from the start of the system operation until the end. The analysis results show the distribution of water content over time, measured hourly from start to finish.

2.5.2. Data Validation

The accuracy of the sensors was evaluated using the Coefficient of Determination R^2 to determine the strength of the linear relationship between the DHT22 sensor readings and the standard reference instrument as shown in Equation 2.

$$R^2 = 1 - \frac{\sum(y_i - \hat{y}_i)^2}{\sum(y_i - \bar{y})^2} \quad (2)$$

The absolute error magnitude of the sensor readings was measured using the Root Mean Square Error (RMSE). This analysis quantifies the average deviation between the sensor's predicted values and the actual reference values, expressed in degrees Celsius (°C) for temperature or percentage (%) for relative humidity as shown in Equation 3.

$$\text{RMSE} = \sqrt{\frac{\sum_{i=1}^{n}(\hat{y}_i - y_i)^2}{n}} \quad (3)$$

where y_i is reference value (standard instrument), $\hat{y}_i$ is measurement value (DHT22 sensor), $\bar{y}$ is mean of the reference values, n is total number of data samples.

3. RESULTS AND DISCUSSION

3.1. Control System Design Results

The structure of the valve used in this system is a duct volume damper made of sheet iron with dimensions of 15 cm × 15 cm. Each duct volume damper is equipped with a DC motor and motor driver to move the valve. One duct volume damper is controlled using a servo motor. All components of the control system work well to regulate air flow through the valve. The valve actuation system, utilizing both DC and servo motors, achieved a 3-second response time for full 90-degree rotations with high positioning reliability. During 15 hours of continuous operation, all units exhibited zero mechanical failures or signal latency, ensuring precise synchronization between the airflow and control logic. The results of the valve control system design can be seen in Figure 7.

(a) (b) (c) (d)

Figure 7. Valve control system design results (a) valve closed by DC motor, (b) valve open by DC motor, (c) valve open 45° by servo motor, (d) valve open 90° by servo motor, 1) Micro limit switch, 2) BTS7960 motor driver, 3) DC worm gear motor, 4) 6A10 diode, 5) Valve, 6) Ducting, 7) DSservo DS3225

3.2. Sensor Calibration Results

Calibration of the DHT22 sensor was performed to evaluate accuracy by comparing the sensor reading (predicted value) with the actual measurement data (true value) using a thermohygrometer. The average calibration results for the eight sensors can be seen in Figure 8. The sensor readings are displayed in actual units, namely temperature in degrees Celsius (°C) and humidity in percent (%), then converted into equilibrium water content (M_e) (%).

Figure 8 shows the average calibration values of the DHT 22 sensor at temperature and humidity. The sensors were formally calibrated within a temperature range of 31 °C to 47 °C and a Relative Humidity (RH) range of 40% to 67%. Although the actual drying process reached extremes of 70 °C and 99% RH, the sensor's reliability across the extended range is justified by the near-perfect linearity shown in the calibration plots, with an R^2 of 0.9998 and regression slopes of 1.0014 for temperature and 0.9962 for RH. These statistical indicators confirm that the DHT22 sensors maintain a highly consistent response, allowing for valid data extrapolation throughout the entire experimental period. The calibration values obtained indicate that the sensor readings compared to the thermohygrometer are accurate because the values obtained are close to 1. This means that the sensor used can function properly. Research (Putri *et al*., 2024; Rustami *et al*., 2022), obtained sensor calibration values with average values of 0.97 and 0.96 for temperature and humidity and 0.9999 and 0.9996 for temperature and humidity. The sensor calibration results demonstrated high

precision for the automated control system. The RMSE for the temperature sensor was 0.47 °C, while the RMSE for the relative humidity sensor was 0.64%. These low RMSE values indicate that the sensors provide reliable real-time data with minimal deviation from reference instruments, ensuring the accuracy of the decision-logic used for airflow management.

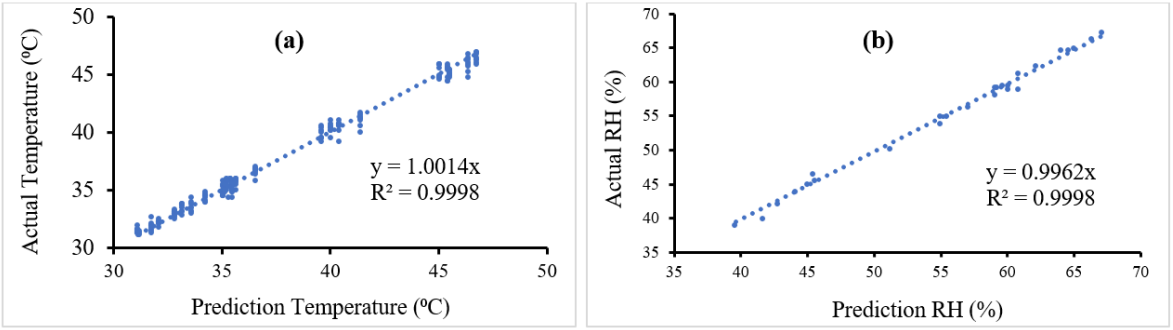

Figure 8. Average calibration graph of the DHT 22 sensor: (a) temperature, (b) humidity

3.3. Control System Performance Testing

3.3.1. Overall System Testing and Analysis

Overall system testing was conducted to evaluate the integrated performance of the control and mechanical components in achieving efficient drying objectives. This test focused on the system's ability to respond automatically to environmental conditions and maintain optimal operating parameters. The test results showed that the designed control system worked effectively, as can be seen in Figure 9. The test data showed that the control system worked effectively in managing air flow through valves and blowers to achieve optimal operating conditions.

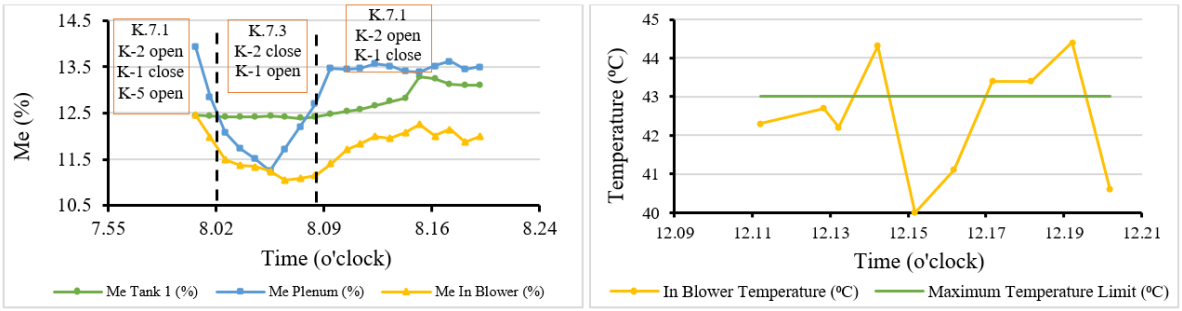

Figure 9. Control system performance testing

Figure 9 illustrates the dynamic responsiveness of the automated control system in managing airflow based on real-time environmental data. Between 08:01 and 08:11 WIB, the system executed selective valve operations driven by the differential between Equilibrium Moisture Content (M_e) in the storage tanks and the plenum. When M_e in Tank 1 was lower than the plenum, Valve 2 opened (Servo at 45°, K.7.1) to introduce dry air and reduce plenum humidity; conversely, the system shifted to a desorption cycle (Servo at 90°, K.7.3) by opening Valve 1 when Tank 1 became more saturated. Simultaneously, the system triggered Valve 5 and the drying blower whenever the inlet air was detected to be drier than the internal dryer environment, ensuring a continuous influx of optimal drying air. Furthermore, Figure 8b demonstrates the temperature regulation mechanism, where Valve 6 automatically modulated ambient air intake to stabilize the blower temperature around a 40–43 °C threshold. This precise modulation is reflected in the overall system efficiency; the thermal performance of the drying system was evaluated using the Drying Air Stability Index, which yielded a value of 3.65. While conventional solar drying operations without automated control modules exhibit high humidity fluctuations of approximately ±17% (Siagian *et al.*, 2025), the current system achieved a much lower

fluctuation with a standard deviation of 8.53%. This represents a 49.82% percentage reduction in humidity fluctuation. Such stability, maintained even during off-sunlight periods, proves the effectiveness of the ESP32-based control logic in regulating the drying air.

3.3.2. Monitoring and Controlling the Temperature and Humidity of the Drying Air

The control system test observation on the dryer was conducted from 08:00 to 17:00 WIB. The data presented is only for one day because it represents the most extreme meteorological conditions, which are very important for testing the adaptive capabilities of the system. These variations made it possible to directly observe and analyze complex technical phenomena that could not be observed on other days. Therefore, this data was the most appropriate choice because it provided strong evidence of the effectiveness and reliability of the control system in facing challenges in the field. The performance of solar dryers is influenced by meteorological conditions, especially ambient air temperature and solar radiation (Gupta *et al*., 2021). The operational precision of the system was quantified through the Average Temperature Deviation, which was recorded at 3.65 °C. This low deviation indicates high thermal consistency within the drying chamber. Consequently, the Control Accuracy Band was maintained at ±3.65 °C, demonstrating the system's ability to suppress external thermal shocks. Variations in the temperature profile of the drying air entering the drying chamber (in blower), hot air exiting the collector (out collector), plenum temperature, and ambient air temperature along with solar radiation data are shown in Figure 10. Figure 10 shows that solar radiation peaks at noon and then decreases. The out collector temperature was recorded between 30.1–65.1 °C and the in blower temperature in the range of 28.8–43.9 °C. The radiation value was recorded between 6–1016.8 W/m^2, while the ambient air temperature was in the range of 28–33.6 °C. These fluctuations affect the variation in the drying air temperature, but with the control system in place, the temperature inside the drying chamber can still be maintained at optimal conditions (Yang *et al*., 2023). Test results consistently prove an inverse relationship between temperature and equilibrium moisture content (M_e). A significant increase in air temperature causes a decrease in M_e values, indicating that the air has greater drying potential. This confirms the important role of automatic control in minimizing the influence of radiation variability on drying quality.

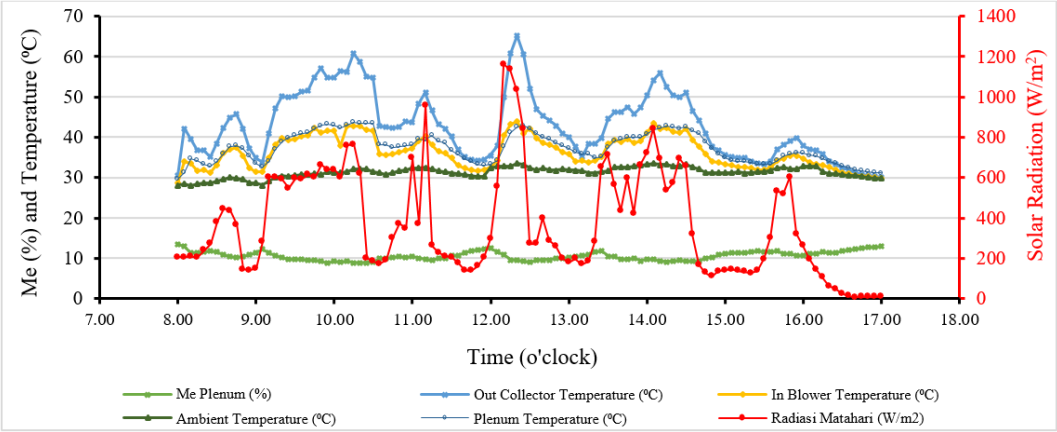

Figure 10. Variations in the air temperature profile during drying

The test was conducted by monitoring the internal temperature of the silica gel stack in tanks 1 and 2, and the ambient temperature can be seen in Figure 11. During the test, heat from tank 1 was actively transferred to the dryer, while tank 2 remained closed. The data shows that the average temperature in tank 2, which was 33.62 °C, was consistently higher than the average temperature in tank 1, which was 31.71 °C. This is an important indicator that tank 2 successfully stored the heat absorbed from the environment without significant heat release for the drying process. The slightly lower temperature in tank 1 shows that the heat energy inside has been successfully transferred to the dryer and can be used for the drying process. The temperature fluctuations in both tanks show a response to the ambient temperature, which averaged 35.06 °C. Tank 1, which actively provides heat, shows a temperature that is influenced by its rate of heat release, while tank 2 represents the thermal capacity of the system when heat is retained. This test proves the important

role of the control system in ensuring effective heat transfer for the drying process, even though the ambient temperature fluctuates. The thermal test results show that despite the fluctuating ambient temperature, the system is able to effectively absorb and store heat energy. The decrease in temperature in the silica gel stack during the day, when the ambient temperature reached its peak, showed that heat energy was absorbed to drive the endothermic desorption process (Musa *et al*., 2025). This proves that the solar drying system works efficiently in utilizing ambient heat energy to dry materials.

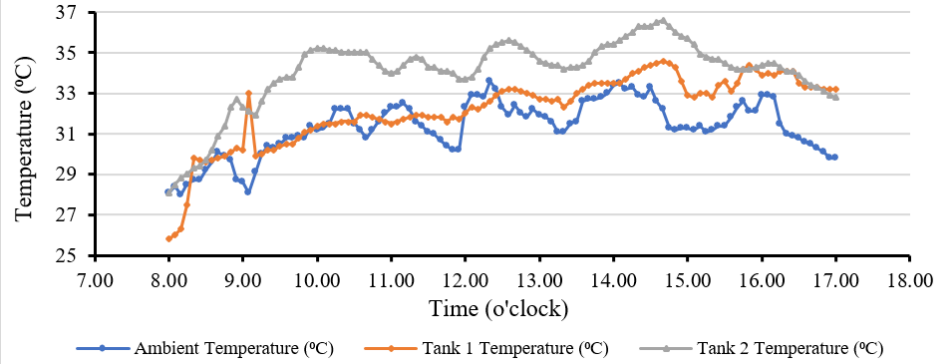

Figure 11. Comparison of ambient temperature with silica gel temperature in the tank

3.3.3. Changes in Silica Gel Moisture Content

Changes in water content in silica gel media show a dynamic response to thermal conditions and air humidity flowing in the system. Variations in equilibrium water content, temperature, and relative humidity of the inlet air play a significant role in regulating the adsorption-desorption equilibrium that occurs in silica gel during the operating period (Hraiech *et al*., 2025), as shown in Figures 12 to 14.

The observations in Figures 12 to 14 show that at 10:00 a.m., the collector temperature reached its peak of 54.80 °C, while the temperature of the silica gel in tanks 1 and 2 also increased to 31.40 °C and 35.20 °C, respectively. The analysis of the silica gel moisture content also showed a decrease in tank 1 from 28.96% to 22.2% and in tank 2 from 27.88% to 22.8% during the daytime period, namely from 08:00 to 14:00 WIB. This shows that even though the incoming air was very hot, the heat energy was used to trigger the desorption process due to the flow of hot and dry air from the collector (Yuliasdini *et al*., 2020), not just to increase the temperature. However, in the afternoon, from 15:00 to 17:00 WIB, the silica gel moisture content increased again. This occurs because the air supply from the collector is stopped, causing adsorption more stable M_e values, indicating that this tank successfully stores heat energy. Fluctuations

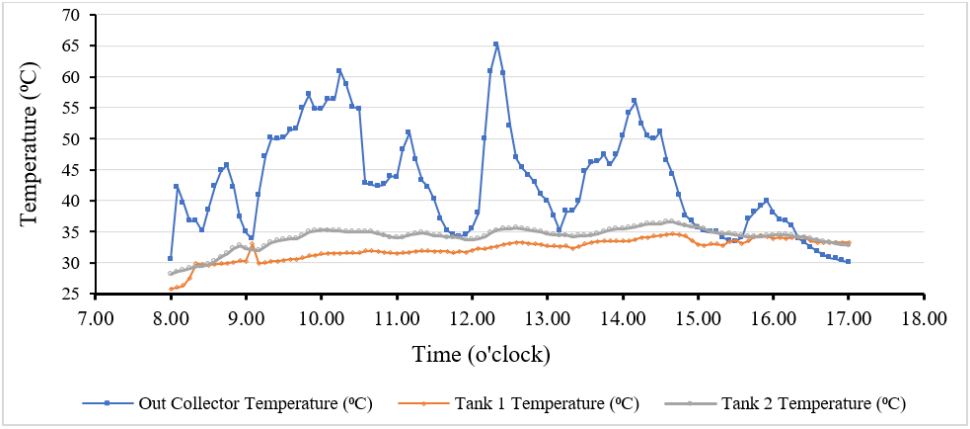

Figure 12. Changes in silica gel tank temperature in response to collector temperature fluctuations

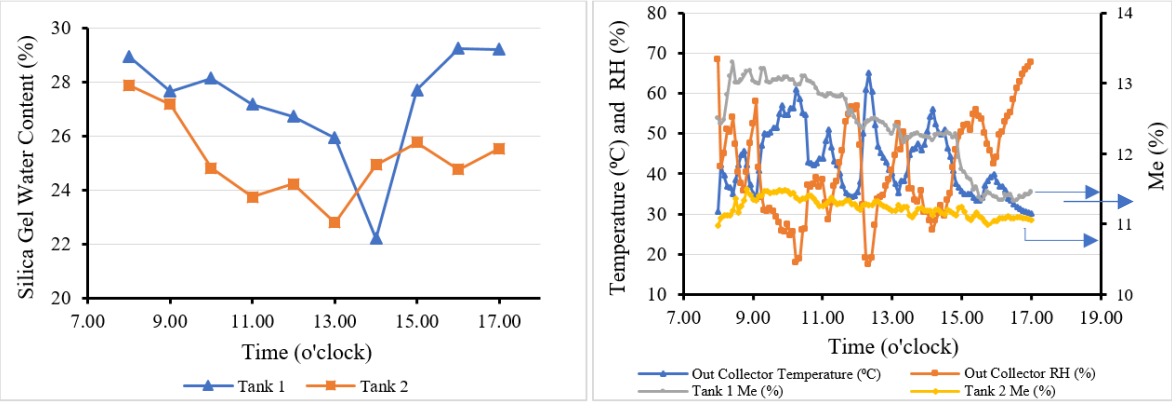

Figure 13. (a) Changes in silica gel water content, and (b) Changes in equilibrium water content (M_e) in the collector and silica gel

in the M_e data for tank 1, such as increases in value at certain times, can be linked to thermal data. This data confirms that the performance of the solar collector is the dominant factor controlling the mass transfer process in silica gel and that the control system plays an important role in maintaining these optimal conditions.

4. CONCLUSIONS

This study successfully implemented an automated airflow control system for a photovoltaic thermal collector integrated with a silica gel adsorption medium. The system demonstrated robust performance in stabilizing the drying microclimate through real-time ESP32-based monitoring and actuation. Key quantitative achievements include a high sensor reliability with an R^2 of 0.9998 and a low thermal RMSE of 0.47 °C. The control system effectively maintained a Drying Air Stability Index of 3.65. Furthermore, the integration of the adsorption channel led to a 49.82% reduction in humidity fluctuation. Despite these results, the study acknowledges certain limitations, specifically its dependence on sensor accuracy for valve triggering and the current small-scale prototype design which may require further optimization for industrial-scale applications. Future research directions should focus on implementing advanced control algorithms, such as PID (Proportional-Integral-Derivative) control or AI-based optimization. Additionally, long-term drying tests on various agricultural products are recommended to evaluate the system's impact on nutritional quality and energy efficiency over extended operational cycles.

AUTHOR CONTRIBUTION STATEMENT

Author	C	M	So	Va	Fo	I	R	D	O	E	Vi	Su	P	Fu
PAO	✓	✓	✓	✓	✓	✓	✓	✓	✓	✓	✓	✓	✓	
LON	✓	✓		✓	✓		✓	✓		✓	✓	✓		✓
IDMS	✓	✓	✓	✓	✓		✓	✓		✓	✓	✓		

C: Conceptualization	Fo: Formal Analysis	O: Writing - Original Draft	Fu: Funding Acquisition
M: Methodology	I: Investigation	E: Writing - Review & Editing	P: Project Administration
So: Software	D: Data Curation	Vi: Visualization	
Va: Validation	R: Resources	Su: Supervision	

REFERENCES

Ayaz, H., Chinnasamy, V., Yong, J., & Cho, H. (2021). Review of technologies and recent advances in low-temperature sorption thermal storage systems. *Energies*, ***14***(19), 1–36. https://doi.org/10.3390/en14196052

Ayisi, E.N., & Fraňa, K. (2020). The design and test for degradation of energy density of a silica gel-based energy storage system using low grade heat for desorption phase. *Energies*, ***13***(17), 4513. https://doi.org/10.3390/en13174513

Gupta, A., Das, B., & Biswas, A. (2021). Performance analysis of stand-alone solar photovoltaic thermal dryer for drying of green chili in hot-humid weather conditions of North-East India. *Journal of Food Process Engineering*, ***44***(6), 13701. https://doi.org/10.1111/jfpe.13701

Hraiech, I., Zallama, B., Belkhiria, S., Zili-Ghedira, L., Maatki, C., Hassen, W., Hadrich, B., & Kolsi, L. (2025). Experimental characterization of silica gel adsorption and desorption isotherms under varying temperature and relative humidity in a fixed bed reactor. *Scientific Reports*, ***15***(1), 29041. https://doi.org/10.1038/s41598-025-14677-7

Jimoh, K.A., Hashim, N., Shamsudin, R., Man, H.C., Jahari, M., & Onwude, D.I. (2023). Recent advances in the drying process of grains. *Food Engineering Reviews*, ***15***(3), 548–576. https://doi.org/10.1007/s12393-023-09333-7

Kazem, H.A., Al-Waeli, A.H.A., Chaichan, M.T., Sopian, K., Al Busaidi, A.S., & Gholami, A. (2023). Photovoltaic-thermal systems applications as dryer for agriculture sector: A review. *Case Studies in Thermal Engineering*, ***47***, 103047. https://doi.org/10.1016/j.csite.2023.103047

Khalil, F.I., Nelwan, L.O., & Subrata, I.D.M. (2016). Desain sistem kendali untuk pengering gabah dengan kolektor surya dan penyimpan panas. *Jurnal Keteknikan Pertanian*, ***4***(1), 87–96.

Kong, D., Wang, Y., Li, M., Keovisar, V., Huang, M., & Yu, Q. (2020). Experimental study of solar photovoltaic/thermal (PV/T) air collector drying performance. *Solar Energy*, ***208***, 978–989. https://doi.org/10.1016/j.solener.2020.08.067

Ludin, N.A., Mustafa, N.I., Hanafiah, M.M., Ibrahim, M.A., Teridi, M.A.M., Sepeai, S., Zaharim, A., & Sopian, K. (2018). Prospects of life cycle assessment of renewable energy from solar photovoltaic technologies: A review. *Renewable and Sustainable Energy Reviews*, ***96***, 11–28. https://doi.org/10.1016/j.rser.2018.07.048

Mitran, R.-A., Ioniță, S., Lincu, D., Berger, D., & Matei, C. (2021). A review of composite phase change materials based on porous silica nanomaterials for latent heat storage applications. *Molecules*, ***26***(1), 241. https://doi.org/10.3390/molecules26010241

Musa, A.A., Nciri, R., & Nasri, F. (2025). Equilibrium moisture effects in silica gel adsorption/desorption. *Engineering, Technology and Applied Science Research*, ***15***(1), 19282–19287. https://doi.org/10.48084/etasr.9207

Nelwan, L.O., Subrata, I.D.M., Yulianto, M., & Suharta, N. (2024). *Pengembangan model sistem pengering surya mandiri dengan metode fotovoltaik-termal (PV/T) dan penyimpanan panas adsorpsi untuk pengeringan gabah* (Laporan penelitian, Program Riset Fundamental). Direktorat Riset dan Inovasi, Institut Pertanian Bogor.

Putra, G.M.D., Lailatun, H.I., Sabani, R., & Setiawati, D.A. (2019). Sistem otomasi photovoltaic pada pembangkit listrik tenaga surya (PLTS) berbasis mikrokontroler Arduino skala lab. *Jurnal Teknik Pertanian Lampung*, ***8***(2), 130–138. https://doi.org/10.23960/jtep-l.v8i2.130-138

Putri, R.E., Arsyafdini, P.O., Putri, I., Arlius, F., & Hasan, A. (2024). Smart tower farming system based on the Internet of Things in greenhouse system. *Tikrit Journal for Agricultural Sciences*, ***24***(3), 228–243. https://doi.org/10.25130/tjas.24.3.18

Rambhad, K.S., Walke, P.V., Kalbande, V.P., Kumbhalkar, M.A., Khond, V.W., Nandanwar, Y., Mohan, M., & Jibhakate, R. (2023). Experimental investigation of desiccant dehumidification with four different combinations of silica gel desiccant wheel on indoor air quality. *SN Applied Sciences*, ***5***(11), 277. https://doi.org/10.1007/s42452-023-05505-6

Rustami, E., Adiati, R.F., Zuhri, M., & Setiawan, A.A. (2022). Uji karakteristik sensor suhu dan kelembaban multi-channel menggunakan platform Internet of Things (IoT). *Berkala Fisika*, ***25***(2), 45–52.

Sadaka, S. (2022). Impact of grain layer thickness on rough rice drying kinetics parameters. *Case Studies in Thermal Engineering*, ***35***, 102026. https://doi.org/10.1016/j.csite.2022.102026

Samykano, M. (2023). Hybrid photovoltaic thermal systems: Present and future feasibilities for industrial and building applications. *Buildings*, ***13***(8), 1950. https://doi.org/10.3390/buildings13081950

Santika, W.G., Anisuzzaman, M., Bahri, P.A., Shafiullah, G.M., Rupf, G.V., & Urmee, T. (2019). From goals to joules: A quantitative approach of interlinkages between energy and the Sustainable Development Goals. *Energy Research & Social Science*, ***50***, 201–214. https://doi.org/10.1016/j.erss.2018.11.016

Siagian, P., Matondang, A.A., Simanjuntak, A.V.H., Kusuma, B.S., Panjaitan, J., & Simanjuntak, A.V.H. (2025). Experimental of environmental development using continuous solar dryer with solid dehumidification for coffee drying. *Journal of Geoscience, Engineering, Environment, and Technology*, ***10***(2), 162–169. https://doi.org/10.25299/jgeet.2025.10.02.21492

Tonadi, E., Niharman, & Wiranto, B. (2024). Performance analysis of solar photovoltaic thermal (PV/T) dryer for drying moringa leaf. *JTTM: Jurnal Terapan Teknik Mesin*, ***5***(1), 90-96. https://doi.org/10.37373/jttm.v5i1.777

Yang, T., Zheng, X., Xiao, H., Shan, C., Yao, X., & Li, Y. (2023). Drying temperature precision control system based on improved neural network PID controller and variable-temperature drying experiment of cantaloupe slices. *Plants*, ***12***(12), 2257. https://doi.org/10.3390/plants12122257

Yuliasdini, N.A., Putri, S.U., Makaminan, T.A., Yuliati, S., & Fadarina. (2020). Efisiensi termal alat pengering tipe tray dryer untuk pengeringan silika gel berbasis ampas tebu. *Prosiding Seminar Mahasiswa Teknik Kimia*, ***1***(1), 29–33.